Research Article
Open Access
CrossMark

Preparation of epitaxial $BiFeO_3$ thin films on Si(001) substrates by pulsed electron deposition

Abstract

To achieve the epitaxial thin films deposition, it is necessary to use properly oriented substrates, with or without buffer layers, matching the lattice parameters of the epitaxial thin film we want to grow. In this work, one-step deposition of epitaxial Bi_2SiO_5(200) and $BiFeO_3$(001) thin films on Si(001) substrates by pulsed electron deposition (PED) technique is reported without special substrate preparation. The deposition of epitaxial BSO(200) and T-BFO(001) directly onto Si(001) substrates during a single target deposition process is relevant and presents enormous potential to reduce costs and improve practicality, interface quality and BFO integration efficiency with Si(001) substrates.

Keywords: A3. Thin Film/Epitaxial Growth; B1. Bismuth compounds; B1. Perovskites; B1. Oxides; B2. Ferroelectric materials; B2. Magnetic materials.

Volume 7 Issue 2 - 2023

Renan M C Ávila,[1] Roney C da Silva,[2,3] Rogério J Prado,[1]
[1]IF / UFMT, Av. Fernando Corrêa da Costa, s/n, Coxipó, Brazil
[2]UNEMAT, Rua A, s/n, Cohab São Raimundo, Brazil
[3]POLITEC, Av. Gonçalo Antunes de Barros, Brazil

Correspondence: Rogério J Prado, IF / UFMT, Av. Fernando Corrêa da Costa, s/n, Coxipó, 78060-900, Cuiabá-MT, Brazil, Email rogerio.prad@ufmt.br

Received: March 13, 2023 | **Published:** April 3, 2023

Introduction

In the last years, ferroelectric materials have been widely studied aiming the development of ferroelectric random-access memories (FeRAM's).[1,2] Also, ferroelectromagnetic materials presenting simultaneous magnetic and electric order, have been widely studied, due to the coexistence of magnetic and electric responses that allows new designs for actuators, transducers and storage devices[3,4] through the use of magnetoelectric switching, i.e., the possibility of reversing the material magnetization by the application of an electric field (or vice-versa). In magnetoelectric random-access memories (MERAM's) it would be possible to combine several advantages as ultrafast (250 ps) electrical writing and non-destructive magnetic reading, combining the best qualities of FeRAM and magnetic resistive RAM (MRAM), what is becoming technically feasible, as pointed out by some authors.[4] By the way, there are limited choices for single-phase materials presenting strong ferro or ferrimagnetic ordering and ferroelectricity.[5,6] Nowadays, ferrite bismuth ($BiFeO_3$ or BFO) is the only known pure material presenting both magnetic and strong ferroelectric effects at room temperature, having a huge impact on the multiferroics field. Besides being a lead-free material, with clear additional benefits ensuring safe usage and future recycling, BFO also presents interesting optical and piezoelectric properties,[4,7,8] opening possibilities for utilization in piezoelectric, magneto-optical or optoelectronic devices.

The bulk BFO crystallographic structure is the rhombohedrally distorted perovskite structure with space group R3c (ICSD Card # 15299; a = 5.588 Å; c = 13.867 Å) shown in figure 1. In BFO, the ferroelectric order is attributed to the Bi^{+3} 6s electrons and the magnetic order is attributed to the Fe^{+3} 3d electrons. A good review on BFO structure, physics and applications, including a phase diagram in function of temperature, is shown in Catalan & Scott (2009) (Figure 1).[4]

Bulk BFO is a commensurate ferroelectric (Curie Temperature, T_C = 1103 K) and an incommensurate antiferromagnet (Néel Temperature, T_N = 643 K) at room temperature,[10,11] due to the long-wavelength (62 nm) spin cycloid existing in the material[11] that makes the linear magnetoelectric effect tend to zero and, indeed, only the quadratic effect has been observed.[12] Anyhow, the linear magnetoelectric effect can be recovered if the spin cycloid is extinguished[13] by applying large magnetic fields, by chemical substitution or by the insertion of epitaxial constraints in the thin films structure.[6,14-16] As large magnetic fields of 20 T are unfeasible in practical magnetoelectric devices, the other two options are usually considered. Since some of these epitaxial BFO(001) films have shown significant magnetization, large electric polarization of about 50-60 μC/cm² in the c direction and strong magnetoelectric coupling,[6] they are promising candidate materials for magnetoelectric device applications.

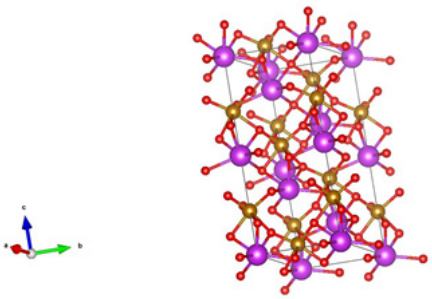

Figure 1 Unit cell of bulk $BiFeO_3$ (ICSD Card # 15299). Red, gold and magenta spheres represent oxygen, iron and bismuth atoms, respectively. Structure drawn using Vesta software.[9]

The BFO thin films deposition may be carried out using low-cost techniques such as spin-coating, liquid phase epitaxy and sol-gel processes,[17-19] however, expensive physical deposition apparatuses as MOCVD, sputtering, MBE or PLD are more often preferred,[20-24] due to the possibility of avoiding contamination and/or improved deposition conditions control. This is precisely the case if the objective is the epitaxial thin films deposition, generally grown onto buffer layers deposited on oriented substrates in deposition processes assisted by high temperature and clean atmosphere/vacuum.

Furthermore, there are still challenges to be overcome for the high quality BFO production, such as obtaining single perovskite phase free of impurities, its tendency to fatigue,[25] bismuth volatilization during annealing, decomposition close to the coercive voltages,[26] and the ferroelectric properties lowering due to high leakage current.[20,25,26] Another important question to be solved is the BFO integration with silicon technologies. In this last challenge, a natural choice for the BFO thin films integration with silicon could be the deposition of a ferroelectric epitaxial BFO thin film on Si(001) substrate.

Particularly, for better integration, an epitaxial phase is desirable due to their improved interface quality and homogeneity[27-29] but, as mentioned before, there are difficulties to achieve that. The epitaxial BFO phase that could be grown directly on Si(001) is T-BFO, a substrate depending[27,30-32] stress-induced metastable pseudo-tetragonal (monoclinic) lattice extremely sensitive to the substrate misfit strain.[31] Pure T-like BFO has only been observed on few substrates structurally but not chemically compatible with Si and/or BFO, including oriented perovskites[20] and hexagonal Al_2O_3.[31,33-35]

Only recently, results found in the literature[27] have shown that integration of BFO with Si(001) is possible when growing T-BFO phase onto a Bi_2SiO_5 (BSO) buffer layer, an oxide chemically and structurally compatible with both Si and T-BFO[36] having Curie temperature (T_C) of 673 K and a relatively large spontaneous polarization in the c direction up to 23.5 μC/cm².[37] Specifically, Zhu et al.[27] found that T-like BFO structure exhibited a true tetragonal symmetry and a memory window up to 6.5 V for an Au/BFO/BSO/Si capacitor with BFO thickness of 135 nm, demonstrating its potentials in the nonvolatile memory applications.

In this research, the BFO thin films deposition by PED is reported, a technique which, according to the authors' knowledge, was not used previously for the deposition of this material. It was found that, in function of the deposition temperature, microcrystalline or epitaxial Bi_2SiO_5 and BFO phases can be obtained onto Si(001) substrates. The present work not only confirms that growth of T-BFO onto a Bi_2SiO_5 (BSO) buffer layer is possible,[27] but also shows that epitaxial BSO(200) and T-BFO(001) can be epitaxially deposited on Si(001) substrates during a single target deposition process, a methodological procedure that can reduce costs and improve practicality, quality and efficiency of BFO integration with Si(001) substrates.

Materials and methods

$BiFeO_3$ thin films were grown on Si(001) substrates using a Neocera PED System of the Thin Films Deposition Laboratory ('*Laboratório de Deposição de Filmes Finos*' - LaDeFF) installed at the Physics Institute of Federal University of Mato Grosso (IF/UFMT – Cuiabá – MT, Brazil). The deposition was performed using a pure $BiFeO_3$ target (from Stanford Advanced Materials, USA), a pulse voltage of 20 kV and ultra-pure (N4.0) O_2 atmosphere (10 mtorr/15 sccm). Deposition temperature on the substrate holder was about 560 °C and 640 °C, respectively for the microcrystalline (BFO1) and epitaxial (BFO2) sample presented in this work. After deposition, sample BFO1 was annealed at about 650 °C for 2 hours.

The X-ray diffraction (XRD) patterns were obtained using a Shimadzu XRD-6000 diffractometer installed at the Multiuser Laboratory of Analytical Techniques ('*Laboratório Multiusuário de Técnicas Analíticas*' – LaMuTA) at the Geosciences School of Federal University of Mato Grosso (FAGEO/UFMT – Cuiabá – MT, Brazil). The diffractometer was equipped with graphite monochromator and conventional Cu tube (0.154178 nm) working at 1.2kW (40 kV - 30 mA) and Bragg-Brentano geometry. A silicon powder was used as standard in order to verify the goniometer alignment and quality of the diffraction data. Errors in the position of the diffraction peaks were verified, being smaller than angular step (0.02°) used during the acquisition. The mean crystallite size of each epitaxial phase, in the out-of-plane direction, was estimated using the Scherrer's equation.[42] Fourier Transform Infrared Spectrometry (FTIR) measurements were performed in a Varian 660 spectrometer, installed at the Physics Institute of Federal University of Mato Grosso (IF/UFMT – Cuiabá – MT, Brazil), on samples grown on Si(001) substrates. The films were measured at room temperature in conventional atmosphere (air), using a resolution of 4 cm^{-1}.

Results and discussion

Figure 2 shows the x-ray diffraction profile of sample BFO1, after annealing at about 650 °C for 2 hours. It is possible to identify the $BiFeO_3$ (ICSD Card # 15299; S.G.: R3c; a = 5.588 Å; c = 13.867 Å) and Bi_2SiO_5 (ICSD Card # 30995; S.G.: $Cmc2_1$; a = 15.173 Å; b = 5.473 Å; c = 5.313 Å) phases. Figure 3 shows the unit cell of the referred Bi_2SiO_5 crystalline structure. The small peak at 28.2° in 2θ, the only peak not corresponding to the BFO or BSO phases in figure 2, is probably due to a small amount of bismuth rich oxide in the sample because Bi_2O_3 (ICSD Card # 15072) has diffraction peaks in this angular range and a Bi_2O_3 like diffraction profile was observed in other BFO samples deposited at lower temperature.

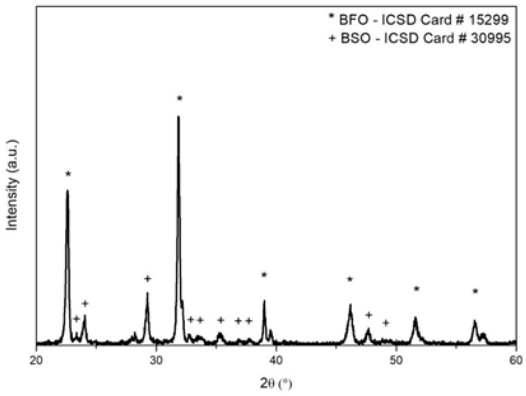

Figure 2 XRD patterns of the BFO1 sample with asterisks (*) and crosses (+) respectively indicating bismuth ferrite (ICSD Card # 15299) and bismuth silicate (ICSD Card # 30995) diffraction peaks.

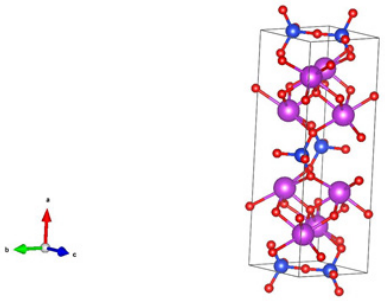

Figure 3 Unit cell of Bi_2SiO_5 (ICSD Card # 30995). Red, blue and magenta spheres represent oxygen, silicon and bismuth atoms, respectively. Structure drawn using Vesta software.[9]

Figure 4 shows the XRD data of the $BiFeO_3$ thin film deposited on Si(001) substrate at approximately 640 °C (Sample BFO2). The diffraction pattern clearly shows that an epitaxial $BiFeO_3$ thin film was successfully grown. One can note the dominant diffraction peaks from epitaxial (001) and (002) crystallographic planes of R-type $BiFeO_3$. Also, one can see the bismuth ferrite diffraction peaks related to the pseudo-tetragonal (T-BFO and T_R-BFO) epitaxial phases.

Due to the identification of nanocrystalline bismuth silicate (Bi_2SiO_5 - ICSD Card # 30995) in sample BFO1, as indicated in Figure 2, it was possible to identify the diffraction peaks from (200), (400) and (600) crystallographic planes in Figure 3, related to the epitaxial growth of bismuth silicate on the Si(001) substrate. Another important peak shown in Figure 3, at 33.0° in 2θ, is caused by the forbidden

Citation: Ávila RMC, da Silva RC, Prado RJ. Preparation of epitaxial $BiFeO_3$ thin films on Si(001) substrates by pulsed electron deposition. *Phys Astron Int J.* 2023;7(2):77–81. DOI: 10.15406/paij.202307.00288

(200) silicon substrate reflection, observed after deposition at high temperature, due to the substrate lattice distortion.[38] The presence of this forbidden peak shows that the silicon substrate atomic structure is distorted during the deposition process, indicating influence of the deposited film on the substrate. Minor diffraction peaks, at 29.3° and 31.8° in 2θ, are also observed. These peaks are related to a small amount of nanocrystalline $BiFeO_3$ and Bi_2SiO_5 phases, being compatible with the main nanocrystalline BSO and BFO peaks shown in figure 2.

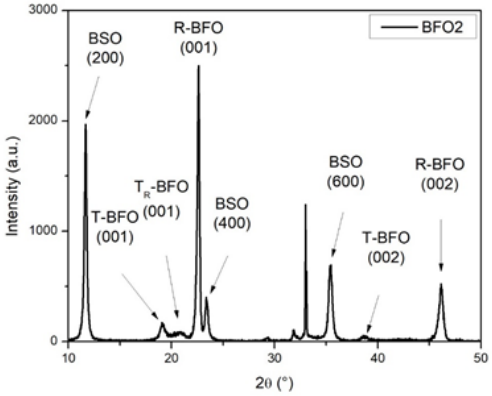

Figure 4 XRD pattern of the epitaxial BFO2 sample, deposited directly on a Si(001) substrate and presenting only BFO(00*l*) and BSO(*h*00) diffraction peaks.

The out-of-plane lattice parameter of the crystalline epitaxial phases determined for the sample BFO2 are 15.20 Å, 4.64 Å, 4.29 Å and 3.93 Å for the epitaxial BSO(200), T-BFO(001), T_R-BFO(001) and R-BFO(001) phases, respectively. In good agreement with previous results found by other authors.[27,30-32] Unfortunately, the determination of the in-plane lattice parameters of these epitaxial phases is not possible with a conventional θ-2θ diffractometer, the equipment used in this work. Anyway, the existence of epitaxial BSO, T-BFO, T_R-BFO and R-BFO in the deposited films is evident and uncontestable.

T-BFO(001) epitaxial phase is reported in the literature as a monoclinic Pm or Pc crystallographic phase (pseudo-tetragonal lattice with a ≈ b ≈ 3.77 Å and c = 4.64 Å). Theoretical and experimental works point that a and b lattice parameters (of the monoclinic lattice) are, approximately, 3.83 Å and 3.71 Å, respectively, but the values found depend on the substrate used [27,30-32]. However, XRD and Raman studies suggest a further change in symmetry, from monoclinic to tetragonal, as film thickness is reduced below 100 nm.[40] In the sample studied here, T-BFO(001) epitaxial phase is represented by the diffraction peak at 19.12° in 2θ (c = 4.64 Å). R-BFO(001) epitaxial phase is monoclinic, presenting pseudo-tetragonal lattice parameters a ≈ b ≈ 3,96 Å and c ≈ 4,04 Å.[30,32] This phase is represented in Figure 4 by the diffraction peaks at 22.60° and 46.13° in 2θ (c = 3.93 Å). The literature data for T_R-BFO(001) epitaxial phase exhibit lattice parameter c = 4.28 Å, with a ≈ b ≈ 3.82 Å.[30] Here, it is represented by the broad diffraction peak at 20.67° (c = 4.29 Å) in Figure 4, among those of T-BFO and R-BFO epitaxial phases. An important point here is that, if T_R-BFO grows between monoclinic T-BFO and R-BFO phases, due to the misfit strain reduction as the thin film thickness increases, the only acceptable possibility is that T_R-BFO lattice is, also, monoclinic. Values of the mean crystallite size found for the BSO(200), T-BFO(001), T_R-BFO(001) and R-BFO(001) phases are 29 nm, 17 nm, 6 nm and 38 nm, respectively.

Silicon from the substrate is necessary to the BSO layer formation, just because there is not another possible source of this chemical element in the system. This necessity indicates that BSO phase is below all BFO phases, that is, in direct contact with the silicon substrate. Some works reported that BSO crystallization occurs at 650 °C,40 in agreement with the deposition temperature for sample BFO2 studied in this work, at about 640 °C. This result shows that bismuth oxide diffused into the silicon (001) substrate, forming an epitaxially oriented BSO(200) buffer layer between the substrate and epitaxial $BiFeO_3$ phases. The oxygen atoms required to obtain the stoichiometric bismuth silicate phase are taken from the oxidized surface of the substrate after exposition to oxygen atmosphere at high temperature, from the material deposited by PED onto the substrate and/or from the O_2 atmosphere used during deposition.

In the early stages of growth, in general, epitaxial BFO thin films present T-BFO phase, followed by T_R-BFO phase when increasing thickness, and finally R-BFO phase.[30] Consequently, it is possible to define the sequence of crystalline epitaxial phases from the substrate to the surface, namely Si(001), BSO(200), T-BFO(001), T_R-BFO(001) and R-BFO(001). As one can see, all these different structures/materials presented peaks in the diffraction pattern shown in Figure 4. In the case of the sample studied in this work, considering the pseudo-tetragonal cell and the expected values (from the literature) of the in-plane lattice parameter for all the epitaxial phases identified in the diffraction profile, it is possible to estimate a contraction of approximately 0.8% from Si(001) to BSO(200) buffer layer (in agreement with the 0.2% elongation observed in the out-of-plane lattice parameter, when compared with the bulk out-of-plane lattice parameter). Normally, when bismuth ferrite is epitaxially grown as a thin film onto, for example, an $SrTiO_3$(001) substrate, the resulting morphology is monoclinic, where the symmetry lowering distortion arises from in-plane contraction and out-of-plane elongation as a result of lattice mismatch between film and substrate, as pointed by several groups.[4] It is also possible to estimate a contraction of approximately 0.5% from BSO(001) to T-BFO(001), an elongation of approximately 0.9% from T-BFO(001) to T_R-BFO(001) phase, and an elongation of approximately 3.9% from T_R-BFO(001) to R-BFO(001). All these variations are acceptable from the experimental and theoretical point of view, for the epitaxial growth of BSO and BFO thin films. According to the literature, transitions from T-BFO to T_R-BFO and/or from T_R-BFO to R-BFO epitaxial phases occur as a function of the film thickness, through stress constraints or stress relaxation mechanisms of the deposited film.[30]

The Bi_2SiO_5 crystalline structure in the a-axis direction consists of an alternating bismuth and silicon oxide layers, as one can see in Figure 3. In the situation of the epitaxial BSO(200) thin film, c-axis direction is in-plane (parallel to the substrate surface and perpendicular to the epitaxial growth direction). Nevertheless, epitaxial BFO(001) phases display a very large spontaneous polarization in the c direction (P_c), but c-axis direction in this case is out-of-plane direction (perpendicular to the substrate surface and parallel to the epitaxial growth direction). Consequently, there is a sample presenting two epitaxial layers with important spontaneous polarization in perpendicular directions, an unusual characteristic in ferroelectric structures, due to necessity of epitaxial growth of both phases to achieve a controlled orientation of the spontaneous polarization, and probably useful for future applications.

The FTIR spectrum of the BFO sample studied in this work is shown in Figure 5. One can see all the typical vibrational modes of Bi_2SiO_5,[41] i.e., Bi-O stretching at 437 cm^{-1}, Bi-O-Si stretching at 854 cm^{-1}, $(SiO_5)^{6-}$ stretching at 945 cm^{-1} and Si-O stretching at 1032 cm^{-}

[1]. The FTIR Bi-O-Si stretching peak at 854 cm^{-1} is only present in samples with nanocrystalline or epitaxial BSO phases detected by XRD and, consequently, in agreement with the XRD data shown in Figure 4.

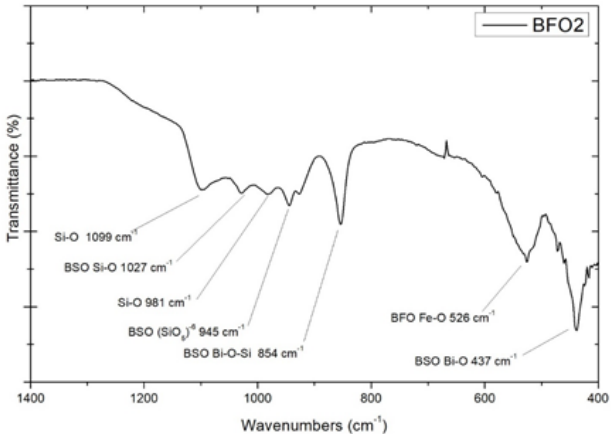

Figure 5 FTIR spectrum of the thin film deposited onto Si(001) substrates.

It is also possible the identification, in Figure 5, of the Fe-O stretching peak at 526 cm^{-1} and Si-O stretching peak at 981 cm^{-1} and 1099 cm^{-1}. This last peak is probably a consequence of the substrate oxidation during deposition in oxygen atmosphere at high temperature. Literature also reports contribution of the bending Fe-O vibrational mode near 437 cm^{-1}, however bending Fe-O vibrations present weak intensity and, consequently, their contribution for the final spectra is small.

Conclusion

The BFO integration with Si(001) substrates is very important to allow the use of BFO with silicon technologies, and the use of epitaxial BFO thin films are desirable due to their improved interface quality and homogeneity.[27-29] As previously cited, there are difficulties integrating epitaxial T-like BFO with Si, and pure T-like BFO has only been observed on a few substrates, including oriented perovskites and hexagonal Al_2O_3 not simultaneously compatible with Si and BFO. Anyway, recent results found in the literature show that integration of the epitaxial T-BFO(001) thin film with the Si(001) substrate is possible if an epitaxial BSO buffer layer is deposited onto the substrate. The bismuth silicate is an oxide chemically and structurally compatible with both Si and T-BFO,[36] obtaining an heterostructure with good potential for nonvolatile memory applications.[27]

In this work, X-ray diffraction shows the growth of the epitaxial BSO, T-BFO, T_R-BFO and R-BFO as a function of the thickness of the deposited film, in the cited order, from the Si(001) substrate to the superficial R-BFO epitaxial phase. FTIR measurements also evidenced the presence of BSO and BFO normal modes of vibration in the deposited heterostructure. After a complete analysis of the experimental data, the results demonstrated that T-like BFO can be epitaxially deposited on Si(001) substrates during a single target deposition process that creates an intermediary Bi_2SiO_5 (BSO) epitaxial layer due to Bi_2O_3 diffusion into the Si substrate. The diffusion of bismuth oxide in the silicon substrate occurs in a large range of temperatures, but the growth of an epitaxial BSO layer occurs, only, if deposition is carried out at an appropriate temperature (~640 °C).

Despite the PED technique used for the thin films deposition studied in this work, the authors consider that similar results can also be obtained using other deposition techniques as sputtering or PLD. The deposition of epitaxial BSO(200) and T-BFO(001) onto Si(001) substrates during a single target deposition process, and without the necessity of a previously deposited buffer layer, is relevant and presents enormous potential to reduce costs and improve practicality, interface quality and efficiency of BFO integration with Si(001) substrates.

Acknowledgements

Authors are grateful to Brazilian funding agencies FAPEMAT ('Fundação de Amparo à Pesquisa do Estado de Mato Grosso') and FINEP ('Financiadora de Estudos e Projetos'), under the FAPEMAT project numbers 850109/2009 and 461812/2009 and FINEP project number 01.04.0121.00, for the acquisition of the apparatuses used in this research. We are also thankful to 'Coordenação de Aperfeiçoamento de Pessoal de Nível Superior' (CAPES, Brazil) for the Ph.D. support of R.M.C. Ávila.

Declarations of interest

None

References

1. T Okamura, M Adachi, T Shiosaki, et al. Epitaxial growth and electrical properties of ferroelectric pb(Zr0.9Ti0.1)O3 films by reactive sputtering. *Jpn J Appl Phys.* 1991;30:1034–1037.
2. T Mihara, H Yoshimori, H Watanabe, et al. Characteristics of Bismuth Layered SrBi2Ta2O9 Thin-Film Capacitors and Comparison with Pb(-Zr,Ti)O3. *Jpn J Appl Phys.* 1995;35:5233–5239.
3. NA Hill. Density functional studies of multiferroic magnetoelectrics. *Annu Rev Mater Res.* 2002;32:1–37.
4. G Catalan, JF Scott. Physics and applications of bismuth ferrite. *Adv Mater.* 2009;21:2463–2485.
5. GA Smolenskii, IE Chupis. Ferroelectromagnets. *Sov Phys Uspekhi.* 1982;25:475–493.
6. J Wang, JB Neaton, H Zheng, et al. Epitaxial BiFeO3 Multiferroic Thin Film Heterostructures. *Science.* 2003;299:1719–1722.
7. SY Yang, LW Martin, SJ Byrnes, et al. Photovoltaic effects in BiFeO3. *Appl Phys Lett.* 2009;25:62909.
8. Kumar RC Rai, NJ Podraza, S Denev, M. et al. Linear and nonlinear optical properties of $BiFeO_3$. *Appl Phys Lett.* 2008;92:121915.
9. K Momma, F Izumi. VESTA3 for three-dimensional visualization of crystal, volumetric and morphology data. *J Appl Crystallogr.* 2011;44:1272–1276.
10. JR Teague, R Gerson, WJ James. Dielectric hysteresis in single crystal $BiFeO_3$. *Solid State Commun.* 1970;8:1073–1074.
11. Sosnowska TP Neumaier, E Steichele. Spiral magnetic ordering in bismuth ferrite. *J Phys C Solid State Phys.* 1982;15:4835–4846.
12. C Tabares-Muñoz, JP Rivera, A Bezinges. Measurement of the Quadratic Magnetoelectric Effect on Single Crystalline $BiFeO_3$. *Jpn J Appl Phys.* 1985;24:1051.
13. W Eerenstein, ND Mathur, JF Scott. Multiferroic and magnetoelectric materials. *Nature.* 2006;442:759–765.
14. YF Popov, AM Kadomtseva, GP Vorob'ev, et al. Discovery of the linear magnetoelectric effect in magnetic ferroelectric BiFeO3 in a strong magnetic field. *Ferroelectrics.* 1994;12:135–140.

15. VA Murashov, DN Rakov, VM Ionov, et al. Magnetoelectric (Bi,Ln) FeO3 compounds: Crystal growth, structure and properties. *Ferroelectrics.* 1994;162:11–21.
16. F Bai, J Wang, M Wuttig, et al. Destruction of spin cycloid in (111) c-oriented BiFeO3 thin films by epitaxial constraint: Enhanced polarization and release of latent magnetization. *Appl Phys Lett.* 2005;86:32511.
17. Y Shirahata, T Oku. Characterization and Photovoltaic Properties of BiFeO3 Thin Films. *Coatings.* 2016;6.
18. X Qi, J Dho, M Blamire. Epitaxial growth of BiFeO3 thin films by LPE and sol–gel methods. *J Magn Magn Mater.* 2004;283:415–421.
19. Y Wang, QH Jiang, HC He, et al. Multiferroic BiFeO3 thin films prepared via a simple sol-gel method. *Appl Phys Lett.* 2006;88:142503.
20. R Rivera, M Hejazi, A Safari. Ferroelectric and dielectric properties of bismuth ferrite based thin films by Pulsed Laser Deposition, in: Proc. ISAF-ECAPD-PFM 2012. 2012:1–4.
21. Vrejoiu M Alexe, D Hesse. Functional Perovskites – From Epitaxial Films to Nanostructured Arrays. *Adv Funct Mater.* 2008;18:3892–3906.
22. JF Ihlefeld, NJ Podraza, ZK Liu, et al. Optical band gap of BiFeO3 grown by molecular-beam epitaxy. *Appl Phys Lett.* 2008;92:142908.
23. C Harnagea, C V Cojocaru, O Gautreau, et al. Piezoresponse force microscopy of PLD-grown multiferroic BiFeO3 films and mesostructures. *Integr Ferroelectr.* 2006;86:1–12.
24. KY Yun, D Ricinschi, T Kanashima, et al. Giant Ferroelectric Polarization Beyond 150 μC/cm2 $BiFeO_3$ Thin Film. *Jpn J Appl Phys.* 2004;43:L647–L648.
25. HW Jang, SH Baek, D Ortiz, et al. Epitaxial (001) BiFeO3 membranes with substantially reduced fatigue and leakage. *Appl Phys Lett.* 2008;92:062910.
26. XJ Lou, CX Yang, TA Tang, et al. Formation of magnetite in bismuth ferrrite under voltage stressing. *Appl Phys Lett.* 2007;90:262908.
27. Zhu Z Yin, Z Fu, Y Zhao, et al. Epitaxial integration of tetragonal BiFeO3 with silicon for nonvolatile memory applications. *J Cryst Growth.* 2017;459:178–184.
28. HN Lee, D Hesse, N Zakharov, et al. Ferroelectric Bi3.25La0.75Ti3O12 Films of Uniform a-Axis Orientation on Silicon Substrates. *Science.* 2002;296:2006–2009.
29. C Dubourdieu, J Bruley, TM Arruda, et al. Switching of ferroelectric polarization in epitaxial $BaTiO_3$ films on silicon without a conducting bottom electrode. *Nat Nanotechnol.* 2013;8:748.
30. Z Fu, ZG Yin, NF Chen, et al. Tetragonal-tetragonal-monoclinic-rhombohedral transition: strain relaxation of heavily compressed $BiFeO_3$ epitaxial thin films. *Appl Phys Lett.* 2014;104:52908.
31. HM Christen, JH Nam, HS Kim, et al. Stress-induced R−MA−MC−T symmetry changes in $BiFeO_3$ films. *Phys Rev B.* 2011;83:144107.
32. W Siemons, GJ MacDougall, AA Aczel, et al. Strain dependence of transition temperatures and structural symmetry of $BiFeO_3$ within the tetragonal-like structure. *Appl Phys Lett.* 2012;101:212901.
33. HJ Liu, HJ Chen, WI Liang, et al. Structural study in highly compressed BiFeO3 epitaxial thin films on $YAlO_3$. *J Appl Phys.* 2012;112:52002.
34. CS Woo, JH Lee, K Chu, et al. Suppression of mixed-phase areas in highly elongated $BiFeO_3$ thin films on NdAlO3 substrates. *Phys Rev B.* 2012;86:54417.
35. YJ Zhao, ZG Yin, XW Zhang, et al. Heteroepitaxy of Tetragonal BiFeO3 on Hexagonal Sapphire(0001). *ACS Appl Mater Interfaces.* 2014;6:2639–2646.
36. Y Wang, CW Nan. Integration of BiFeO3 thin films on Si wafer via a simple sol–gel method. *Thin Solid Films.* 2009;517:4484–4487.
37. Y Kim, J Kim, A Fujiwara, et al. Hierarchical dielectric orders in layered ferroelectrics $Bi_2Si_2O_5$. *IUCrJ.* 2014;1:160–164.
38. Zhao M Steinhart, M Yosef, SK Lee, et al. Lithium Niobate Microtubes within Ordered Macroporous Silicon by Templated Thermolysis of a Single Source Precursor. Chem Mater. 2005;17:3–5.
39. H Béa, M Bibes, S Petit, et al. Structural distortion and magnetism of BiFeO3 epitaxial thin films: a Raman spectroscopy and neutron diffraction study. Philos Mag Lett. 2007;87:165–174.
40. Yamaguchi Y. Preparation of bismuth titanate thin films by alternately supplying metal-organic-decomposition method. J Korean Phys Soc. 2003;42:408–S1411.
41. XJ Dai, YS Luo, SY Fu, et al. Facile hydrothermal synthesis of 3D hierarchical Bi2SiO5 nanoflowers and their luminescent properties. Solid State Sci. 2010;12:637–642.
42. Guinier. X-Ray Diffraction in Crystals, Imperfect Crystals and Amorphous Bodies, 1st Ed., Dover, New York, 1994, pp. 142–143.

Citation: Ávila RMC, da Silva RC, Prado RJ. Preparation of epitaxial $BiFeO_3$ thin films on Si(001) substrates by pulsed electron deposition. *Phys Astron Int J.* 2023;7(2):77–81. DOI: 10.15406/paij.202307.00288